Title

New Constraints on the Continuum Emission Mechanism of Active Galactic Nuclei: Intensive Monitoring of NGC 7469 in the X-Ray and Ultraviolet

Journal

The Astrophysical Journal, 505(2)

ISSN

0004-637X

Authors

Nandra, K
Clavel, J
Edelson, RA
et al.

Publication Date

1998-10-01

DOI

10.1086/306181

Peer reviewed

NEW CONSTRAINTS ON THE CONTINUUM-EMISSION MECHANISM OF AGN: INTENSIVE MONITORING OF NGC 7469 IN THE X-RAY AND ULTRAVIOLET

K. Nandra[1,2], J. Clavel[3], R.A. Edelson[4], I.M. George[1,5], M.A. Malkan[6], R.F. Mushotzky[1], B.M. Peterson[7] and T.J. Turner[1,5]

ABSTRACT

We have undertaken near-continuous monitoring of the Seyfert 1 galaxy NGC 7469 in the X-ray with *RXTE* over a ~ 30 d baseline. The source shows strong variability with a root-mean-square (rms) amplitude of ~ 16 per cent, and peak–to–peak variations of a factor of order 2. Simultaneous data over this period were obtained in the ultraviolet (UV) using *IUE*, making this the most intensive X-ray UV/X-ray variability campaign performed for any active galaxy.

Comparison of the continuum light curves reveals very similar amplitudes of variability, but different variability characteristics, with the X–rays showing much more rapid variations. The data are not strongly correlated at zero lag. The largest absolute value of the correlation coefficient occurs for an anticorrelation between the two bands, with the X-ray variations leading the UV by ~ 4 d. The largest positive correlation is for the ultraviolet to lead the X-rays by ~ 4 d. Neither option appears to be compatible with any simple interband transfer function. The peak positive correlation at ~ 4d occurs because the more prominent peaks in the UV light curve appear to lead those in the X-rays by this amount. However, the minima of the light curves are near-simultaneous. These observations provide new constraints on theoretical models of the central

[1]Laboratory for High Energy Astrophysics, Code 660, NASA/Goddard Space Flight Center, Greenbelt, MD 20771

[2]NAS/NRC Research Associate

[3]ISO Observatory, European Space Agency. Apartado 50727, 28080 Madrid, Spain

[4]X-ray Astronomy Group, Department of Physics and Astronomy, University of Leicester, University Road, Leicester, LE1 7RH, United Kingdom

[5]Universities Space Research Association

[6]Department of Astronomy, University of California, Los Angeles,CA 90024

[7]Department of Astronomy, The Ohio State University, 174 West 18th Avenue, Columbus, OH 43210

regions of active galactic nuclei. Models in which the observed UV emission is produced solely by re-radiation of absorber X-rays are ruled out by our data, as are those in which the X-rays are produced solely by Compton upscattering of the observed UV component by a constant distribution of particles. New or more complex models must be sought to explain the data. We require at least two variability mechanisms, which have no simple relationship. We briefly explore means by which these observations could be reconciled with theoretical models.

Subject headings: galaxies:active – galaxies: nuclei – galaxies: individual (NGC 7469) – ultraviolet: galaxies – X-rays: galaxies

1. INTRODUCTION

The origin of the continuum emission of Active Galactic Nuclei (AGN) – which covers an extremely broad band – is not well understood. In a number of high luminosity sources, it appears that this emission peaks in the ultraviolet (UV), the so-called "Big Blue Bump" (Shields 1978; Malkan & Sargent 1982). Strong, and apparently non-thermal X-ray flux is also a persistent property of AGN (e.g., Marshall et al. 1981). The X-ray emission covers a wide band from at least 0.1-100 keV, and can be described by a power-law form (Mushotzky, Done & Pounds 1993).

The Big Blue Bump is often identified as the thermal output of an accretion disk (henceforth the accretion disk model e.g., Shakura & Sunyaev 1973). Heat is generated by viscous dissipation in the disk, which then radiates in the optical/UV regime for black hole masses typical of AGN (e.g., Sun & Malkan 1989). An alternative origin for the UV continuum emissions has been suggested by both observational and theoretical considerations. Guilbert & Rees (1988) postulated that the UV need not be internally generated in the accretion disk, but could arise via absorption and thermal re-emission (hereafter referred to as "thermal reprocessing") of X-rays in optically thick gas close to the central engine. The material - which could be but does not necessarily have to be the disk – would imprint features on the X-ray spectra (e.g., Lightman & White 1988; George & Fabian 1991; Matt, Perola & Piro 1991). Such features have been found (e.g., Nandra & Pounds 1994) and suggest that approximately half of the incident X-rays are absorbed in the optically thick material. Spectroscopic observations of strong gravitational and Doppler effects in the iron Kα line profiles of Seyfert galaxies (e.g., Tanaka et al. 1995; Nandra et al. 1997) suggest that this material lies extremely close to the central black hole and is

probably in the form of a disk (Fabian et al. 1995). The bulk of the continuum photons absorbed in the gas should then be re-emitted at the characteristic thermal temperature of the material. For dense gas close to the central engine, and particularly for "standard" accretion disks, this should be in the optical/UV.

Most models for the X–ray continuum of AGN are based on the idea that lower-energy photons are Compton scattered by a population of hot electrons and/or pairs (which we refer to as "upscattering" models e.g., Sunyaev & Titarchuk 1980; Svensson 1983; Guilbert, Fabian & Rees 1983). The seed photons are often assumed to be those in the blue bump. Specific models differ primarily in their assumptions about, e.g., the geometry of the system (e.g. Haardt & Maraschi 1991, 1993; Haardt, Maraschi & Ghisellini 1994; Stern et al. 1995), the question of whether the electron population has a thermal or non-thermal distribution, the importance of pairs (e.g., Zdziarski et al. 1990, 1994).

These models have been successful in explaining various observations. The goal underlying the exploration of the models is the discovery of the process responsible for the generation of the copious energy output of AGN. While the case for accreting supermassive black holes is becoming compelling, the method by which the rest-mass energy of the material is converted into radiative energy is still highly uncertain. Some specific questions which remain about the emission mechanisms include:

1. How important is viscous dissipation in the generation of the UV?
2. What proportion of the UV arises via thermal reprocessing of X–rays?
3. What is the seed population for upscattering into the X–rays?
4. What mechanism accelerates the particles which up-scatter these seed photons?

A powerful way of investigating these questions is by variability campaigns. These have already reaped rich rewards in the study of AGN emission lines via "reverberation mapping" (e.g. Peterson 1993, Netzer & Peterson 1997, and references therein). These emission line campaigns, however, also had strong implications for the generation of the continua, which we shall discuss below. The models discussed above all imply strong connections between the continuum emission in different bands. For example, the accretion disk emission could cover an extremely broad band, depending on the temperature profile of the disk. The thermal reprocessing model predicts that the X-rays should be generating UV emission. The upscattering model suggests the converse. By observing the variability in these bands, therefore, we can make inferences as to which of the various processes is in operation and to what degree. In particular, simultaneous X-ray/UV data should be the most revealing.

A number of AGN have been monitored simultaneously at optical/UV and X-ray energies. Leaving aside blazars, the best-studied sources are NGC 4151, NGC 5548 and NGC 4051. In the first two objects, there is evidence for a correlation between the two bands. The best-sampled (and therefore most reliable) case is NGC 4151, in which the 1455 Å and 2–10 keV flux appears to correlate well on all time scales from hours to a year (Perola et al. 1986; Edelson et al. 1996). In NGC 5548, the flux in the two bands is also well correlated on time scales from days to 1 year (Clavel et al. 1992). In both sources however, the correlation appears to break down during one very large UV outburst. NGC 4051 shows different behavior, in that the X-ray emission showed large-amplitude (factor ~ 2) variability, while the optical emission remained steady to within a few per cent when observed over a ~ 2 d baseline (Done et al. 1990). For completeness, we also mention the results obtained for other non-blazar AGN, though their significance is marginal due to the small number of simultaneous observations and/or the short duration of the campaigns. In Fairall 9, the slow decline of the 2–10 keV flux mimics the secular fading of the UV and optical continuum from 1978 to 1985 (Morini et al. 1986). The UV-optical versus X-ray flux correlation seems to hold in NGC 4593 (Santos-Lléo et al. 1995), whereas in MCG-8-11-11 (Treves et al. 1990), 3C120 (Maraschi et al. 1991) and 3C 273 (Courvoisier et al. 1990) the two wavebands appear to be independent of each other. These previous attempts at determining the relationship between the components have obviously left some ambiguity. This is perhaps not surprising as generally the sampling of the light curves has been rather poor.

In order to provide an improved dataset, a campaign of near-continuous *RXTE* and *IUE* monitoring of NGC 7469 was undertaken over a ~ 1 month baseline. The results of the campaign in terms of the relationship of the X-ray and UV variability are the subject of this paper. We have effectively divided the paper into two halves. Sections 2-4 discuss the observational results exclusively, which are then summarized in Section 5. Section 6 then investigates the implications of the observational results within the framework of the models discussed above and suggest possible ways of reconciling the data with models.

2. OBSERVATIONS

Full details of the *IUE* data analysis and reduction, and the nature of the UV variability has been described in Wanders et al. (1997; hereafter W97). Here we provide details of the X-ray observations, made with the *RXTE* Proportional Counter Array (PCA). The *RXTE*/HEXTE data will be presented elsewhere.

NGC 7469 was observed by *RXTE* for a ~ 30 d period beginning 1996 June 10 02:26:40

UT. The nominal observational strategy was to observe once-per *RXTE* orbit ($\sim$ 90 min) with a 1.5 ks exposure. In practice the exposure time in each orbit varied, with some orbits containing no useful data, and others with up to 4ks of good data. Approximately 10d into the campaign operations switched to one observation every other orbit due to satellite power constraints. We utilized the so-called `STANDARD-2` data mode which provides a minimum time resolution of 16s, full detector and layer identification and full spectral information. Due to temperature fluctuations and arcing, 2 of the 5 proportional counter units (PCU's) which make up the PCA were occasionally turned off during the campaign. For simplicity and consistency here we only consider data for those three PCU's (PCU0, PCU1, PCU2) which were operating throughout, and quote all count rates for the sum of these three detectors. Some details of the *RXTE* PCA in-orbit performance can be found in Jahoda et al. (1996).

2.1. Data reduction

Initial data reduction proceeded on the `STANDARD-2` event files by creating time filters based on various housekeeping parameters. These are listed in Table 1. Briefly, these criteria were used to reject earth-occulted data and data contaminated by the earth's limb, to exclude periods when the pointing position of the satellite was unacceptable, and to reject anomalous background events due to electrons. After applying these criteria we combined all the `STANDARD-2` data into a single light curve, restricting the pulse-height range to obtain only the counts in the 2-10 keV band of the first of the three layers, where the PCA is most sensitive. We obtained 593 ks of acceptable data in total.

2.2. Background subtraction

Background subtraction is the most important consideration when analyzing *RXTE* data for relatively weak sources such as NGC 7469. The PCA has no simultaneous background monitoring and therefore a model background must be constructed based on various housekeeping parameters. The *RXTE* background model is still evolving, but the current implementation consists of three components: particle-induced background, activation in the South Atlantic Anomaly (SAA), and the diffuse X-ray background.

The particle-induced components are modeled by analyzing earth data from throughout the mission. The main particle component is found to be well correlated with many of the PCA anti-coincidence rates, which are used to flag and veto non X-ray events. Many such

rates are available and the current model uses the so-called "Q6" rate, which measures coincidences which fire 6 of the 8 PCU anode chains. In addition to this primary particle component, the satellite's passage through the SAA induces radioactive decay terms into the background. These can be accounted for by correlating the positional history of the satellite with the PCA count rate during occultation. The sky background is determined by subtracting the predicted particle components from "blank" sky pointings, averaging over several positions. The mean background rate predicted for our observation was 10.79 ct s^{-1} for the top layers of the three detectors in the 2-10 keV band.

As our interest is in the X-ray variability of the source in the 2-10 keV band, point-to-point fluctuations in the diffuse X-ray background – being constant in time – will not affect our conclusions regarding the variability. More serious are potential inaccuracies in the modeling of the particle background which is variable on a wide range of (potentially characteristic) time scales. Therefore, to test the accuracy of the background model at our epoch we accumulated the earth-occulted data obtained during our campaign and applied the particle background model. This analysis allows us to test systematic uncertainties in the background subtraction, as with a perfect predictive model the mean of this light curve should be consistent with zero, and the variance in the data should be due only to photon counting statistics. We did find variance in this light curve, however, which we attribute to imperfect modeling of the background. The magnitude of the excess variance depends on the binning time scale. Fig. 1 shows the background-subtracted source and earth-occulted light curves, with a bin size of 512s. Note that no earth-occulted datum is plotted after day 272 as after this time, large flares are apparent (~ 60 ct s^{-1} peak). The origin of this behavior is unknown, but a detailed examination of these periods reveals that the count rate begins to flare *only* when the Earth elevation angle becomes less than zero, which strongly indicates that they are a phenomenon associated with pointing at the earth. The background-subtracted source data do not show such flares, and the housekeeping data do not show unusual values during this time period. We therefore conclude that this phenomenon does not affect our light curve of NGC 7469.

Even when these data are excluded, the background-subtracted light curve of the earth-occulted data shows long term trends, which are currently not accounted for in the background model. Excluding the flaring periods, we obtained a mean value of 0.032 ± 0.010 ct s^{-1} and estimate a variability amplitude of 0.24 ct s^{-1} (1σ) in the background with a time binning of 512s. This systematic error was added in quadrature to the statistical error for each data point in the source light curve. In spite of the systematic nature of these errors, which makes them difficult to propagate correctly, the variations in the source-minus-background light curve are so large that we conclude that they are intrinsic to NGC 7469. This is amply demonstrated by comparing the excess variability in the

earth-occulted data to the source variations in the same energy band of 1.38 ct s^{-1}, a factor ~ 6 larger, and an examination of Fig. 1.

3. INTERBAND CONTINUUM RELATIONSHIPS

After background subtraction, the mean source count rate was found to be 8.67 ± 0.01 ct s^{-1} in the 2-10 keV band (statistical error only), which corresponds to a flux of $\sim 3.4 \times 10^{-11}$ erg cm^{-2} s^{-1} assuming the *ASCA* spectrum for this source given by George et al. (1998). The corresponding 2-10 keV luminosity is 4.2×10^{43} erg s^{-1} ($z = 0.017$; we have assumed $H_0 = 50$ and $q_0 = 0.5$). Fig. 2 shows the background-subtracted X-ray light curve of NGC 7469 in the 2-10 keV band, in 512s bins, which has been normalized to this mean count rate. There are clearly strong variations on many time scales, and we find a fractional rms variability parameter $F_{\rm var} = 0.16$, defined as the square root of the excess variance of the data points, divided by the mean (e.g., Rodriguez-Pascual et al., 1997). Variability information is detailed in Table 2. This shows the number of data points, $N_{\rm data}$ in each light curve, $F_{\rm i}(t)$. The mean flux $\overline{F}$, defined as

$$\overline{F} = \frac{1}{N_{\rm data}} \sum_{i=1}^{N_{\rm data}} F_{\rm i}(t)$$

The standard deviations of the points $\sigma_{\rm F}$ is also shown, defined by:

$$\sigma_{\rm F}^2 = \frac{1}{N_{\rm data} - 1} \sum_{i=1}^{N_{\rm data}} (F_{\rm i}(t) - \overline{F})^2$$

The data points $F_{\rm i}(t)$ have associated error bars $\sigma_i(t)$ and we define the expected variance due to random errors as,

$$\Delta_{\rm F}^2 = \frac{1}{N_{\rm data}} \sum_{i=1}^{N_{\rm data}} \sigma_i^2(t)$$

Then, we define the excess variance $\sigma_{\rm XS}$ as the difference between the observed and expected variances,

$$\sigma_{\rm XS}^2 = \sigma_{\rm F}^2 - \Delta_{\rm F}^2$$

and the rms variability parameter as,

$$F_{\rm var} = \sigma_{\rm XS}/\overline{F}$$

From Fig. 2 it can be seen that the minimum-to-maximum variations are roughly a factor ~ 2. Note that normalized count rate has been plotted in Fig 2, rather than the flux. This can cause some additional uncertainty if the spectrum is strongly variable. We defer a full discussion of the X-ray spectrum of NGC 7469 and its variability to a later paper, but a preliminary examination of the hardness ratio suggests that there are no strong spectral changes during our observation.

The normalized *IUE* continuum light curve at 1315Å (W97) is also shown in Fig. 2 (filled squares). Several things are apparent from a comparison of these two plots. The most striking result of our simultaneous campaign is that the X-ray and UV fluxes are not well correlated at zero lag. We also note with interest that the amplitude of variations in the X-ray and UV are very similar, with $F_{\rm var}$ in the two bands of 0.16 and 0.15 respectively (Table 2). These values are dominated by the events on long time scales, which have the largest amplitude. It is tempting to match up the largest amplitude peaks and troughs in the two light curves and conclude that there is a significant correlation, but with a time-delay between the two bands. The large-amplitude trends in the light curves show two relatively well-defined maxima and minima. However, the data are clearly inconsistent with a single or simple time delay. The maxima show an apparent (and similar) delay of ~ 4 d between the UV and X-ray, but the minima appear to occur simultaneously. We investigate this further below. There are also some highly significant and very rapid events in the X-ray light curve which are not seen with the same amplitude in the UV (e.g., the events around days 252 and 255).

3.1. Auto-correlation functions

We have calculated the auto-correlation functions (ACFs) of the two light curves and show these in Fig. 3. Before performing these correlations, the UV light curve at 1315Å was truncated to cover the same time-span as the X-ray campaign. Furthermore, to provide the fairest comparison, we resampled the X-ray light curve to have the same time resolution as the UV light curve. The X-ray auto–correlation function is clearly narrower than that of the UV continuum and has more structure. The Full-Width at Half Maximum (FWHM) of the X-ray ACF is 1.7d, whereas the UV ACF has FWHM more than twice this (5.3d). This shows that the X-rays have more variability on short time scales. The ACFs are subject to some uncertainty due to the length of the data-train, but we feel this is unlikely to be a major problem in our analysis. For example, if we compare the ACF of the full

UV light curve presented by W97 (which lasts ~ 45d) to the truncated version, we obtain very similar values for the FWHM of the UV ACF. We are therefore confident that the comparison of the FWHM is not strongly affected by the sampling of the two light curves.

3.2. Cross-correlation analysis

We have correlated the X-ray and UV continuum light curves using two techniques for purposes of comparison, a cross-correlation with interpolation (ICCF: Gaskell & Peterson 1987; White & Peterson 1994), and the z-transformed Discrete Correlation Function (ZDCF: Edelson & Krolik 1988; Alexander 1997). We have evaluated the correlation coefficient for delays in the range $-15 < D < 15$ d computing the values in steps of 0.1 d for the ICCF. The ZDCF binning is described in Alexander (1997) but in practice was similar to the ICCF. The results of this cross-correlation analysis are shown in the top panel of Fig. 4. The two methods are in good agreement. Fig. 5 shows the fluxes plotted against one another, using a linear interpolation in the X-ray light curves to estimate the X-ray flux at the time of the UV observations. These demonstrate the conclusion which is already apparent by eye, that the light curves are not well-correlated at zero lag. Using the ZDCF, and a linear fit to nearby points, we estimate a correlation coefficient, r, at zero lag of $r_0 = 0.19$ (see also Table 3). Assuming that the pairs of X-ray/UV data points in the cross correlation are independent, this implies a significant correlation at ~ 96 per cent confidence. A local fit to the ICCF near zero lag gives a slightly smaller estimate for the correlation coefficient of $r_0 = 0.16$. This value of r is not significant. We conclude that the two bands are not strongly correlated at zero lag.

Peaks and troughs are apparent in Fig. 4. The most significant value of r is negative, implying an anti-correlation between the bands when the X-ray variations lead those in the UV by $D \sim 4$ d. A local Gaussian fit to the ZDCF shows a minimum correlation coefficient of $r^-_{\rm max} = -0.57$. Assuming the data points are independent, the formal significance of obtaining this by chance is $p_{\rm r} = 8 \times 10^{-9}$, after accounting for the number of trials. The most significant positive correlation when the X-ray variations lag those in the UV by $D \sim 4$ d. A Gaussian fit to the ZDCF here gives a maximum value for the correlation coefficient of $r^+_{\rm max} = 0.45$ (Table 3). After accounting for the number of trials, the probability of obtaining such a coefficient by chance is found to be $p_{\rm r} = 2 \times 10^{-4}$, assuming independent data points. The ICCF gives very similar values.

On the face of it, it seems possible to conclude either that the X-ray and UV light curves show a significant anti-correlation, with the X-ray variations leading the UV by $D \sim 4$ d, or that two bands are correlated, with the UV emission leading the X-rays by a

similar amount. However, the interpretation of these possible lags is unclear and we note that having sampled so few of the highest amplitude "events" with our baseline, aliasing problems are possible. Also, as already noted above, the character of the two light curves shown in Fig. 2 shows that it is highly unlikely that the data would be consistent with a single lag.

If one component were driving the other, a more complex relationship between the two bands may be expected, depending on factors such as the geometry of the system. In optical/UV reverberation studies, this relationship is characterized by the "transfer function" (Blandford & McKee 1982). Once again, however, it seems difficult to reconcile our data with a single transfer function. In any simple and/or constant geometry (and therefore transfer function) the variations in the secondary band should lag those of the driver with a delay which was similar for all "events".

3.3. Power-density spectra

Besides measuring the auto-correlation functions and interband cross-correlation function, as has been done in the previous sections, the statistical characteristics of the UV and X-ray variations can be compared by measuring the fluctuation power density spectra (PDS) in the different bands. This is made more powerful in this case because it is the first time that simultaneous, quasi-continuously sampled data have been obtained for any AGN on such long time scales. This means that the PDS can be compared directly without having to worry that the source was varying differently at different times, or about the effects of different sampling patterns. This is also the first measurement with relatively evenly-sampled data of the X-ray PDS of a Seyfert galaxy on time scales longer than a few days.

For this analysis, both the UV and X-ray light curves were slightly resampled to yield 128 data points centered on identical times. The X-ray data were rebinned directly into 20947 sec intervals. The rebinned UV light curve was constructed by interpolating the measured light curve to the mid-point times used in the rebinned X-ray light curve. Both light curves were renormalized by subtracting the mean and dividing by the standard deviation of the points. These data were then Fourier transformed with a Parzen window (Press et al. 1992), with the results shown in Fig. 6.

As expected, both the UV and X-ray PDS show no narrow features that would be indicative of periodic or quasi-periodic variability, but instead the fluctuation power rises strongly to lower frequencies. This "red noise" PDS is a well-established feature

of AGN (e.g., Krolik et al. 1991; Lawrence & Papadakis 1993; Green, McHardy & Lehto 1993). *EXOSAT* observations yielded PDS characterized over the frequency range $10^{-3} < f < 10^{-5}$ Hz as $f^{-1.5}$ for most Seyfert galaxies (Green et al. 1993; Lawrence & Papadakis 1993), although the slopes must flatten out to lower temporal frequencies or the total power will diverge. However, estimating the slopes for our power spectra is complicated for two reasons. First, there are insufficient points to re-bin the PDS and therefore assign error bars to the points using the method of, e.g. Papadakis & Lawrence (1993). Second, the noise level due to statistical fluctuations, particularly for the UV light curve, is difficult to estimate. Regarding this latter point, we have performed simulations of constant light curves, with the same sampling patterns as the interpolated light curves used to produce the power spectra. Gaussian noise was added to these assuming the mean error bars of the points to estimate the distribution. These were then Fourier transformed, giving us an estimate of the noise level predicted by the error bars. In the case of the X-ray PDS, we find a predicted noise level which is a factor ~ 2 lower than the mean power at the high frequency end of the PDS. Conversely, the UV noise level is a factor ~ 2 *higher* than the observed power at high frequencies. This suggests that the UV error bars are overestimated. Indeed, W97 point out that their conservative method of calculating the UV error bars will tend to produce upper limits. A good estimate of the slope of the UV PDS would require a more reliable estimate of the noise level.

We note that the X-ray PDS clearly shows more power than the UV across the whole range of temporal frequencies. This is difficult to reconcile with the fact the the $F_{\rm var}$ values, which should represent the integral of the PDS over some frequency range, are so similar. As seen in Fig. 6, the X-ray PDS appears to be only slightly flatter than the UV PDS. Naively, the observed variability might lead one to predict that the X-ray PDS had a much flatter slope, given clear eyeball evidence for more rapid variability. As noted above, statistical noise could have a strong effect on the UV PDS, accounting for the bulk of the high frequency power and making the PDS appear flatter. However, these problems make it difficult to make a meaningful statements regarding these preliminary PDS.

4. CONTINUUM-LINE RELATIONSHIPS

W97 have also presented the light curves of the UV emission lines obtained during the *IUE* campaign, and performed cross correlations of their fluxes with the 1315Å continuum. As found for the original campaign on NGC 5548 (Clavel et al. 1991; Peterson et al. 1991), the line fluxes were found to lag those of the continuum by a few days. Here we examine the relationship of the X-ray flux with that of the UV emission lines. Table 2

shows the variability parameters for the emission lines. Interestingly, we find that many of the emission lines are reasonably well correlated with the X-ray continuum close to zero lag. Fig. 4 also shows the ZDCF and ICCF correlation functions for the X-ray versus the prominent UV emission lines and Table 3 shows the correlation coefficients. Once again, we truncated the *IUE* light curves such that they cover the same time as the X-ray data. We find that the Lyα, N v and C iv lines are all correlated better with the X-ray continuum than the UV continuum at zero lag. However, an examination of the peak correlation coefficients shows that if a time delay is allowed, the UV continuum is better correlated with all of the emission lines (Table 3).

5. OBSERVATIONAL SUMMARY

Here we summarize our observational results:

1. The UV and X-ray continua of NGC 7469 varied by a factor ~ 2 peak-to-peak on time scales of ~ 10 d
2. The X-rays also showed much more rapid variations (~ 50 per cent in ~ 1 d, which were not observed in the UV
3. The variations in the two bands are not well correlated at zero lag
4. The strongest peaks in the X-ray light curve are delayed by ~ 4 d with respect to those in the UV
5. The prominent "troughs" in the light curves are near-simultaneous
6. The highest absolute value of the correlation coefficient occurs for an X-ray lead of ~ 4d and an anticorrelation between the bands
7. The strongest positive correlation occurs for an X-ray lag of ~ 4 d
8. Many of the prominent UV emission lines are better correlated with the X-ray continuum at zero lag, but they are all better correlated with the UV emission when a lag is allowed

6. DISCUSSION

We have investigated the relationship between the X-ray and UV emission in NGC 7469 on time scales of hours-weeks. The poor correlation between the X-ray and UV light

curves at zero lag may be considered a surprising result because, as mentioned in §1, some previous experiments suggested a good correlation, and little if any time lag between the variations in the two bands (e.g. NGC 5548, NGC 4151). No other AGN, however, has been monitored as intensively and for such a long duration.

Variability information has important implications for the physical mechanisms responsible for the production of the X-ray and UV emission in AGN. If the flux changes in two bands are correlated, this suggests some causal link between them. A time lag between the bands then shows which component drives the other. If X-ray variations lead those in the UV, this is strongly suggestive of thermal reprocessing. If the opposite is observed, this strongly favors upscattering. With a simple transfer function this delay should be similar for all "events" in the light curve. No such simple behavior was observed during our campaign and the interpretation is less straightforward. Our data require modifications to the simplest ideas about the emission mechanisms in the UV and X-ray.

6.1. Model ingredients

It is widely accepted that the radiative energy from AGN originates as the rest-mass energy of accreting material. The conversion process must include a mechanism to accelerate the particles which produce the X-rays as they are the highest-energy photons to carry an appreciable fraction of the luminosity. In principle, the remainder of the AGN spectrum could be produced by thermal reprocessing following absorption of some fraction of this X-ray continuum. Viscous dissipation in the accretion flow, however, could dominate the observed UV emission. In many scenarios there is also a radiative connection between the UV and X-ray emission regions: X-rays can be produced by upscattering of UV seed photons and UV emission can be produced by re-radiation of absorbed X-rays. In these circumstances, a substantial number of factors can affect the observed variability:

1. Changes in the physical properties (e.g. optical depth, temperature, geometry) of the particle distribution which produces the X-rays
2. Instabilities in the accretion flow
3. The geometry and size of the X-ray and UV emission regions
4. Anisotropy of the radiation fields, which might include relativistic effects close to the black hole
5. The temperature distribution of the absorbing medium

6. The importance of feedback, in which variations in each band affect the other

7. Changes in occulting/absorbing media

6.2. Implications of the NGC 7469 data

Our data have a number of implications for the processes which produce the UV–to–X-ray emissions of NGC 7469 and the observed variability, which we now discuss. First we consider our observations in the context of historical data and the spectral energy distribution of NGC 7469.

6.2.1. The broad-band perspective

The mean X-ray and UV fluxes observed for NGC 7469 during our campaign are very much typical of the respective historical means for this source. The mean flux in the 2–10 keV band, based on historical observations over the period 1979-1993, is $\sim 3 \times 10^{-11}$ erg cm^{-2} s^{-1}. Furthermore, the range of historical variability is very similar to that observed during our campaign. This suggests that we sampled a large fraction of source variability in NGC 7469 during our one-month campaign, although we observe no obvious flattening of the PDS (Fig. 6) at the lowest frequencies. Chapman, Geller and Huchra (1985) derived a mean value of 4.6×10^{-14} erg cm^{-2} s^{-1} Å^{-1} for the 1430–1460 Å continuum flux of NGC 7469 from 10 *IUE* observations in 1979–1982. Similarly, Edelson, Pike and Krolik (1990), reported a mean value of 4.8×10^{-14} erg cm^{-2} s^{-1} Å^{-1} for the continuum flux at 1450 Å (rest wavelength) from 16 *IUE* observations in 1979–1985. With a mean UV flux at 1485 Å (observed wavelength) of 4.0×10^{-14} erg cm^{-2} s^{-1} Å^{-1} (W97), NGC 7469 was thus neither particularly faint nor exceptionally bright during our campaign. The optical–to–X-ray spectral index of NGC 7469, $\alpha_{ox} = 1.22$, is not significantly different from that of, e.g., NGC 5548 ($\alpha_{ox} = 1.25$), or the mean index for Seyfert galaxies (Kriss, Canizares and Ricker 1980).

The spectral energy distribution of NGC 7469 is shown in Fig. 7. The only real peculiarity of NGC 7469 is the presence of a circumnuclear starburst ring within 1.″5 of its nucleus. Genzel et al. (1995) estimate that the starburst accounts for two-thirds of the source bolometric luminosity and it may dominate the IR emission. However, it only contributes 4 percent to the observed X-ray flux (Perez-Olea and Colina 1996). The starburst should be invariant on the time scales sampled here and have no effect on the X–ray/UV variability.

6.2.2. The X–ray continuum

The presence of rapid variations in the X-rays which are not seen in the UV implies that the particle distribution responsible for the X-rays is variable. The X-ray emission mechanism is highly uncertain, but as mentioned in the introduction, many models have concentrated on Compton upscattering of seed UV photons by a population of hot electrons and/or pairs (e.g. Haardt & Maraschi 1991, 1993). Our observations show that if the observed UV photons are the seed population, then the rapid variations of the X-rays do not arise from variations in the seed. Either the optical depth, temperature or geometry of the upscattering region must be changing. In the latter case, changes in the distribution of active regions in the X-ray source, or kinematic effects can produce variability (e.g., Abramowicz et al. 1991; Haardt, Maraschi & Ghisellini 1997).

Longer-term variations are also observed in the X-ray flux and these could also arise from processes such as those just mentioned. The fact that the power spectrum shows no obvious features or break is supportive of this interpretation. The fluctuations have a similar amplitude to those in the UV and this suggests a connection between the bands. This is intriguing. One possibility is that the long time-scale variability in the X–rays is due to changes in the UV seed population. In the simplest such interpretation - where the upscattering region is point-like and lies in the line of sight to a point-like seed source we expect a 1:1 correlation between the two bands with no lag. This is ruled out by our data, although we note that the minima appear to be very close in time. In more complex geometries, there may be time lags which will be in the sense that the X-ray variations follow those in the UV. The delay of ~ 4 d between the peaks is superficial evidence in favor of upscattering. In that model, however, we expect the lag to be very short, being dependent primarily on the light travel time between the regions, modified by geometrical factors. A lag of ~ 4 d, the only plausible conclusion here, seems rather long to be associated with these processes. In addition, we are unable to envisage a purely geometrical modification of a linear process which accounts for *both* the relationship between the maxima and that of the minima.

6.2.3. The UV continuum

We now consider the alternative that the X-ray emission drives the UV in the thermal reprocessing scenario. The luminosities in the X-ray and UV bands are similar (Fig. 7) and thermal reprocessing can therefore be energetically important. As stated above, the 2-10 keV observed flux of NGC 7469 at our epoch was 3.4×10^{-11} erg cm^{-2} s^{-1}. However, the X-ray emission of NGC 7469 covers a far wider band than this, with significant emission

being observed down to ~ 0.1 keV with ROSAT (Brandt et al. 1993) and most likely up to at least 100 keV as seen by OSSE (Zdziarski et al. 1995; Gondek et al. 1996). Estimates of the underlying photon index of the continuum are in the range $1.9 - 2.0$ after accounting for the effects of Compton reflection (Piro et al. 1990; Nandra & Pounds 1994). We estimate the mean X–ray luminosity of NGC 7469 at our epoch to be $1.8 \times 10^{44}\,\mathrm{erg\ s^{-1}}$ in the 0.1-100 keV band. In the canonical thermal–reprocessing scenario about half of this luminosity should be absorbed in the accretion disk or other material. After estimating that fraction which is Compton scattered rather than absorbed (George & Fabian 1991) we conclude that the presence of the iron emission line and reflection hump in NGC 7469 indicate that a luminosity of $\sim 8 \times 10^{43}\,\mathrm{erg\ s^{-1}}$ of the X-ray emission of NGC 7469 is reprocessed and re-emerges as thermal emission.

Let us now suppose that all of this luminosity emerges in a single black body (which represents the narrowest physically-realistic spectrum) peaking close to 1315Å ($kT \sim 2$ eV). Such a blackbody is almost sufficient to account for the continuum at 1315Å (Figure 7). Therefore, it is energetically possible that reprocessed X-rays produce some of the observed UV continuum and its variations. As in the case of upscattering, the simplest thermal reprocessing models predict a strong positive correlation between the bands, with any time lags being in the sense that the X-ray variations lead those in the UV. No such lag is observed. We do find that the strongest *anti*–correlation of the datasets occurs for the X-rays leading the UV, but the interpretation of such a result is far from obvious and we do not comment on it further.

Even if aliasing has caused us to "miss" a positive correlation with a long (~ 14 d) lag between the UV and X–rays, any lag longer than a day or so is very difficult to explain. Any single transfer function which related the two bands would smooth the light curve of the responding band and reduce its amplitude. We observe, however, that the amplitudes of variability on long time scales are very similar. We therefore reject such a possibility. In this case it is even more difficult to envisage a complex geometry which can reproduce the light curves.

It therefore seems highly unlikely that any substantial proportion of the 1315Å continuum of NGC 7469 arises from thermal reprocessing unless, for example, there is substantial anisotropy of the X-ray emission. W97 found that the variations at longer UV wavelengths followed those at shorter wavelengths, but with a time lag of a fraction of a day. Collier et al. (1998) have demonstrated that this trend continues into the optical, and Peterson et al. (1998) find this trend to be significant at no less than the 97 per cent confidence level. This, together with the rapidity of the variations in NGC 7469, is most easily explicable in terms of the thermal reprocessing hypothesis. However, our data

essentially rule out models in which all the observed optical/UV flux is re-radiated X-ray emission. The optical/UV variability therefore requires either intra-band reprocessing, which is difficult from an energetics standpoint, or some other model.

Should we therefore conclude that the UV/optical continuum in NGC 7469 arises from direct emission by the accretion disk? Our data offer no direct constraints on accretion disk models, as no explicit relationship between the X–ray and UV emissions is predicted by those models. Nonetheless, the fact that thermal reprocessing is strongly disfavored by our data has profound implications for the disk models. The rapid and wavelength-coherent variations in the optical and UV flux of AGN is difficult to reconcile with a standard α-disk (e.g. Krolik et al. 1991; Molendi, Maraschi & Stella 1992). Prior to our observations, it was conceivable that thermal reprocessing was responsible for these rapid variations. There is now a clear need for a revision of accretion disk theory to account for these wavelength-independent variations without resorting to reprocessing.

6.2.4. The extreme ultraviolet (EUV) continuum and UV emission lines

Given the presence of a typical iron Kα line and reflection hump in this source (Piro et al. 1990; Nandra & Pounds 1994) we are left with the question of where the putative reprocessed X-ray flux is emitted. One possibility is that the thermal reprocessing occurs in a molecular torus (Ghisellini, Haardt & Matt 1994; Krolik, Madau & Zycki 1994), in which case it might emerge in the infrared. Such an hypothesis would predict a narrow iron Kα line in the X-ray spectrum, whereas in many Seyfert galaxies these lines are extremely broad. The case of NGC 7469 is unclear, with Guainazzi et al. (1994) finding no evidence for a broad component and Nandra et al. (1997) finding marginal evidence. A conclusive determination requires a longer exposure with *ASCA*, but it seems highly likely that the iron Kα line and Compton hump in Seyfert 1 galaxies in general are produced extremely close to the central black hole (e.g., Nandra et al. 1997). We would therefore expect the reprocessed emission to emerge at a higher energy. As shown above, however, the thermally reprocessed X-rays only make a strong contribution to the observed optical and UV wavebands if the emission is strongly peaked at those wavelengths. It seems more likely that the emission covers a range of temperatures, in which case the reprocessed flux would be difficult to detect when spread over a wide band.

Alternatively, it could peak in the (unobserved) EUV band. Figure 7 shows that this can indeed be the case. A blackbody of luminosity $8 \times 10^{43}\,\mathrm{erg\ s^{-1}}$ contributes less than 5 per cent of the flux at 1315 Å as long as $kT > 12$ eV. Intensity variations in such a component would be undetectable with *IUE*. Similarly, the *ASCA* spectrum constrains

$kT < 60$ eV. If the spectral form is broader than a single blackbody, the range of allowed temperatures is correspondingly wider. Interestingly, Brandt et al. (1993) reported evidence for a soft excess in the *ROSAT*/PSPC data which can be modeled as a blackbody of $kT \sim 110$ eV and a luminosity of 10^{43} erg s^{-1}. This can be identified with the high energy tail of such a broad, reprocessed component.

The major UV emission lines are excited by unobservable EUV photons. An extrapolation of the X-ray spectrum observed by *ASCA* (George et al. 1998) and of the UV spectrum into that band indicate roughly equal contributions at energies at which the lines are excited. With the two components being poorly correlated at zero lag, it is therefore difficult to determine which will be the dominant EUV component at any given time. We have suggested above that there may even be a third contributor to the EUV, the reprocessed X-rays. In other words, the shape of the ionizing continuum changes with time. This effect could account for certain difficulties which have been encountered in explaining the emission line responses to the observed UV continuum in reverberation mapping experiments. Our observations suggest that the unseen EUV continuum is not directly related to the observed *IUE* flux, which therefore cannot be assumed to be a perfect representation of the continuum driving the line emission. It is also interesting to note that the emission-line light curves show long term trends which are not apparent in the continuum bands. This is most clearly demonstrated by Fig. 8, which shows the X-ray and UV continuum light curves, together with those of the Lyα and CIV emission lines. These have all been renormalized to the $F_{\rm var}$ value and thus the y-axes crudely represent the number of standard deviations from the mean. Both emission lines clearly show a long-term reduction in their flux which is not seen in either continuum.

6.3. Steps towards a new model

In the light of the above, it is clear that new or more complex models must be sought to explain the data which have been obtained thus far, and particularly those described in this paper. Here we suggest some ways in which our new data might be reconciled with the existing paradigm by modification or extension. We emphasize that such a discussion is incomplete and *ad-hoc*.

As we have stated above, it seems most likely that the X–ray flux which is absorbed when the iron Kα lines is being generated emerges in a relatively weak, broad component, that may peak the EUV/soft X-ray band. The emission in this band may well provide the crucial connection between the higher and lower-energy components. A reasonable interpretation of the longer-timescale variability observed in our light curve is that the UV

emission leads that in the X-rays, but with a variable lag. This suggests the dominant source of variations is in the seed population of an upscattering model. We do, however, bear in mind the caveat that the particle distribution of the upscattering medium must also be variable, to produce the most rapid variations. To explain the "variable" time lag, we suggest that there are multiple "seed" populations, which dominate at different times. In particular we suggest that the main source of 1315Å photons is located at a distance of ~ 4 lt d from the X–ray source and they are the dominant seed population when the source is in a high flux state, thus introducing a 4d "lag" between the X-rays and UV. When the 1315Å flux is observed to decline, however, this allows other emitting regions to dominate the seed distribution. In particular we suggest at these times that EUV/soft X-ray photons are the dominant seed population. They arise from closer in and are therefore observed to have little or no lag with the X-rays.

As might be apparent from the above discussion, the primary X–rays, reprocessed X-rays and primary UV might well exist in a rather fine balance in the typical AGN. Future observational data on other objects of similar quality to that presented here, and preferably including the far-UV and soft X-ray bands, will be necessary for further progress and to establish the generality of the phenomena explored here.

We thank the *RXTE* team for their operation of the satellite, the *RXTE* GOF for their assistance in data analysis, Keith Jahoda and Mike Stark for their extensive work on the background subtraction. We also thank Tal Alexander and Shai Kaspi for assistance with the ZDCF, Hagai Netzer and Iossif Papadakis for discussions, and the anonymous referee for many helpful suggestions. We acknowledge the financial support of the National Research Council (KN) and Universities Space Research Association (IMG,TJT). We are grateful for the support of this work through NASA grants NAG5-3233 and NAG5-3497 to Ohio State University. This research has made use of the Simbad database, operated at CDS, Strasbourg, France; of the NASA/IPAC Extragalactic database (NED) which is operated by the Jet Propulsion Laboratory, Caltech, under contract with NASA; and of data obtained through the HEASARC on-line service, provided by NASA/GSFC.

Table 1. *RXTE* selection criteria

Criterion	Description
`OFFSET < 0.01`	Angular offset from nominal pointing position (°)
`ELV > 10`	Angle from earth's limb (°)
`NUM_PCU_ON > 2`	Number of operational PCUs
`(VpX1L+VpX1R)/Q6 < 0.1`	Normalized propane layer veto rate

Note. — Only data from PCUs 0,1 and 2 were employed; VpX1L represents the veto rate between the PCA propane layer and the left half of the Xenon layer; VpX1R is for the right half of the Xenon layer; Q6 represents the veto rate between 6 of the 8 anode chains in the PCA

Table 2. Variability parameters

Band	$N_{\rm data}$	$\overline{F}$	$\sigma_{\rm F}$	$\Delta_{\rm F}$	$\sigma_{\rm XS}$	$F_{\rm var}$
2-10 keV	1513	8.59	1.41	0.47	1.33	0.155
1315 Å	123	4.38	0.66	0.16	0.65	0.147
Lyα	121	203.3	17.5	7.99	15.5	0.076
N V	123	38.5	7.04	6.22	3.28	0.085
Si IV	123	54.9	11.4	9.60	6.13	0.112
C IV	123	271.9	19.0	10.6	15.7	0.057
He II	123	65.9	13.6	13.2	3.39	0.051
C III	123	60.5	8.94	15.1	···	···

Note. — The UV light curves have been truncated to cover the same baseline as the X-ray light curve. $N_{\rm data}$ is the number of data points; $\overline{F}$ is the mean flux in ct s^{-1} for the X-ray and in units of 10^{-14} erg cm^{-2} s^{-1} Å^{-1} for the UV; $\sigma_{\rm F}$ is the square root of the variance of the light curve. $\Delta_{\rm F}$ is the mean error bar; $\sigma_{\rm XS}$ is the square root of the excess variance and $F_{\rm var}$ is the square root of the normalized excess variance, which we term the rms variability parameter (see text)

Table 3. Correlation coefficients

Band	r_0	$r^+_{\rm max}$	$r^-_{\rm max}$
Correlations with the X-ray light curve			
1315 Å	0.19	0.45	-0.57
Lyα	0.28	0.35	-0.35
N V	0.24	0.26	-0.24
Si IV	0.22	0.23	-0.37
C IV	0.30	0.39	-0.33
He II	0.14	0.18	-0.24
Correlations with the truncated UV light curve			
2-10 keV	0.18	0.46	-0.59
Lyα	0.25	0.56	-0.32
N V	0.18	0.41	-0.21
Si IV	0.35	0.53	-0.29
C IV	0.20	0.49	-0.36
He II	0.38	0.42	-0.30

Note. — r_0 is the correlation coefficient between X-ray or truncated UV and the other component at zero lag; $r^+_{\rm max}$ is the maximum (*positive*) correlation coefficient in the range $\pm$10 d; $r^-_{\rm max}$ is the minimum (*negative*) correlation coefficient in that range

REFERENCES

Abramowicz, M.A., Bao, G., Lanza, A., Zhang, X.-H., 1991, A&A, 245, 454

Alexander, T., 1997, in "Astronomical Time Series", D. Maoz, A. Sternberg, E. Leibowitz, Eds, Kluwer, Dordrecht, p. 163

Blandford, R.D., McKee, C.F., 1982, ApJ, 255, 419

Brandt, W.N., Fabian, A.C., Nandra, K., Tsuruta, S., 1993, MNRAS, 265, 996

Chapman, G.N.F., Geller, M.J., Huchra, J.P., 1985, ApJ, 297, 151

Clavel, J., et al., 1991, ApJ, 366, 64

Clavel, J., et al., 1992, ApJ, 393, 113

Collier, S., et al. 1998, ApJ, in press

Courvoisier, T. J.-L., et al., 1990, A&A, 234, 73

Courvoisier, T., J.-L., Clavel, J., 1991, A&A, 248, 389

Done, C., Ward, M.J., Fabian, A.C., Kunieda, H., Tsuruta, S., Lawrence, A., Smith, M.G., Wamsteker, W., 1990, MNRAS, 243, 713

Edelson, R.A., Krolik, J.H., 1987, ApJ, 333, 646

Edelson, R.A., Malkan, M.A., 1986, ApJ, 308, 59

Edelson, R.A., Pike, G.F., Krolik, J.H., 1990, ApJ, 359, 86

Edelson, R.A., et al., 1996, ApJ, 470, 364

Fabian, A.C., Nandra, K., Reynolds, C.S., Brandt, W.N., Otani, C., Tanaka, Y., Inoue, H., Iwasawa, K., 1995, MNRAS, 277, L11

Gaskell, C.M., Peterson, B.M., 1987, ApJS, 65, 1

Genzel, R., Weitzel, L., Tacconi-Garman, L.E., Blietz, M., Cameron, M., Krabbe, A., Lutz, D., Sternberg, A., 1995, ApJ, 444, 129

George, I.M., Fabian, A.C., 1991, MNRAS, 249, 352

George, I.M., Turner, T.J., Netzer, H., Nandra, K., Mushotzky, R.F., Yaqoob, T., 1998, ApJS, 114, 73

Ghisellini, G., Haardt, F., Matt, G., 1994, MNRAS, 267, 743

Gondek, D., Zdziarski, A.A., Johnson, W.N., George, I.M., McNaron-Brown, K., Magdziarz, P., Smith, D., Gruber, D.E., 1996, MNRAS, 282, 646

Green, A.R., McHardy, I.M., Lehto, H.J., 1993, MNRAS, 265, 664

Guainazzi, M., Matsuoka, M., Piro, L., Mihara, T., Yamauchi, M., 1994, ApJ, 436, L35

Guilbert, P.W., Fabian, A.C., Rees, M.J., 1983, MNRAS, 205, 593

Guilbert, P.W., Rees, M.J., 1988, MNRAS, 233, 475

Haardt, F., Maraschi, L., 1991, ApJ, 380, 51

Haardt, F., Maraschi, L., 1993, ApJ, 413, 507

Haardt, F., Maraschi, L., Ghisellini, G., 1994, ApJ, 432, L95

Haardt, F., Maraschi, L., Ghisellini, G., 1997, ApJ, 476, 620

Jahoda, K., Swank, J.H., Giles, A.B., Stark, M.J., Strohmayer, T., Zhang, W., Morgan, E.H., 1996, EUV, X-ray and Gamma-ray Instrumentation for Space Astronomy VII, O. H. W. Siegmund and M. A. Grummin, Eds., SPIE 2808, p. 59

Kriss, G.A., Canizares, C.R., Ricker, G.R., 1980, ApJ, 242, 492

Krolik, J.H., Horne, K., Kallman, T.R., Malkan, M.A., Edelson, R.A., Kriss, G.A., 1991, ApJ, 371, 541

Krolik, J.H., Madau, P., Zycki, P.T., 1994, ApJ, 420, L57

Lawrence, A., Papadakis, I., 1993, ApJ, 414, L85

Lightman, A.P., White, T.R., 1988, ApJ, 335, 57

Malkan, M.A., Sargent, W.L., 1982, ApJ, 254, 22

Maoz, D., Netzer, H., 1989, MNRAS, 236, 21

Maraschi, L., Chiappetti, L., Falomo, R., Garilli, B., Malkan, M.A., Tagliaferri, G., Tanzi, E.G., Treves, A., 1991, ApJ, 368, 138

Marshall, N., Warwick, R.S., Pounds, K.A., 1981, MNRAS, 194, 987

Matt, G., Perola, G.C., Piro, L., 1991, A&A, 245, 63

Molendi, S., Maraschi, L., Stella, L., 1992, MNRAS, 255, 27

Morini, M., et al., 1986, ApJ, 307, 486

Mushotzky, R.F., Done, C., Pounds, K.A., 1993, ARAA, 31, 717

Nandra, K., Pounds, K.A., 1994, MNRAS, 268, 405

Nandra, K., George, I.M., Mushotzky, R.F., Turner, T.J., Yaqoob, T., 1997, ApJ, 477, 602

Netzer, H., Peterson, B.M., 1997, in Astronomical Time Series, ed. D. Maoz, A. Sternberg, E.M. Leibowitz (Dordrecht: Kluwer), p. 85

Papadakis, I., Lawrence, A., 1993, MNRAS, 261, 612

Perez-Olea, D.E., Colina, L., 1995, ApJ, 468, 191,

Perola, G.C., et al., 1986, ApJ, 306, 508

Peterson, B.M., 1993, PASP, 105, 247

Peterson, B.M., et al., 1991, ApJ, 368, 119

Peterson, B.M., Wanders, I., Horne, K., Collier, S., Alexander, T., Kaspi, S., Maoz, D., 1998, PASP, in press

Piro, L., Yamauchi, M., Matsuoka, M., 1990, ApJ, 360, L35

Press, W.H., Teukolsky, S.A., Vetterling, W.T., Flannery, B.P., 1992, *Numerical Recipes*, Cambridge University Press, Cambridge, UK

Rodriguez-Pascual, P.M., et al., 1997, ApJS, 110, 9

Santos-Lleó, M., Clavel, J., Barr, P., Glass, I.S., Pelat, D., Peterson, B.M., Reichert, G.A., 1995, MNRAS, 274, 1

Shakura, N.I., Sunyaev, R.A., 1973, A&A, 24, 337

Shields, G.A, 1978, Nature, 272, 706

Stern, B.E., Poutanen, J., Svensson, R., Sikora, M., Begelman, M.C., 1995, ApJ, 449, L13

Sun, W.-H., Malkan, M.A., 1989, ApJ, 346, 68

Sunyaev, R.A., Titarchuk, L.G., 1980, A&A, 86, 121

Svensson, R., 1983, ApJ, 270, 300

Tanaka, Y., et al., 1995, Nature, 375, 659

Treves, A., Bonelli, G., Chiappetti, L., Falomo, R., Maraschi, L., Tagliaferri, G., Tanzi, E.G., 1990, ApJ, 359, 98

Wanders, I., et al., 1997, ApJS, 113, 69

White, R.J., Peterson, B.M., 1994, PASP, 106, 879

Zdziarski, A.A., Fabian, A.C., Nandra, K., Celotti, A., Rees, M.J., Done, C., Coppi, P.S., Madejski, G.M., 1994, MNRAS¡ 269, L55

Zdziarski, A.A., Ghisellini, G.G., George, I.M., Fabian, A.C., Svensson, R., Done, C., 1990, ApJ, 363, L1

Zdziarski, A.A., Johnson, W.N., Done, C., Smith, D., McNaron-Brown, K., 1995, ApJ, 438, L63

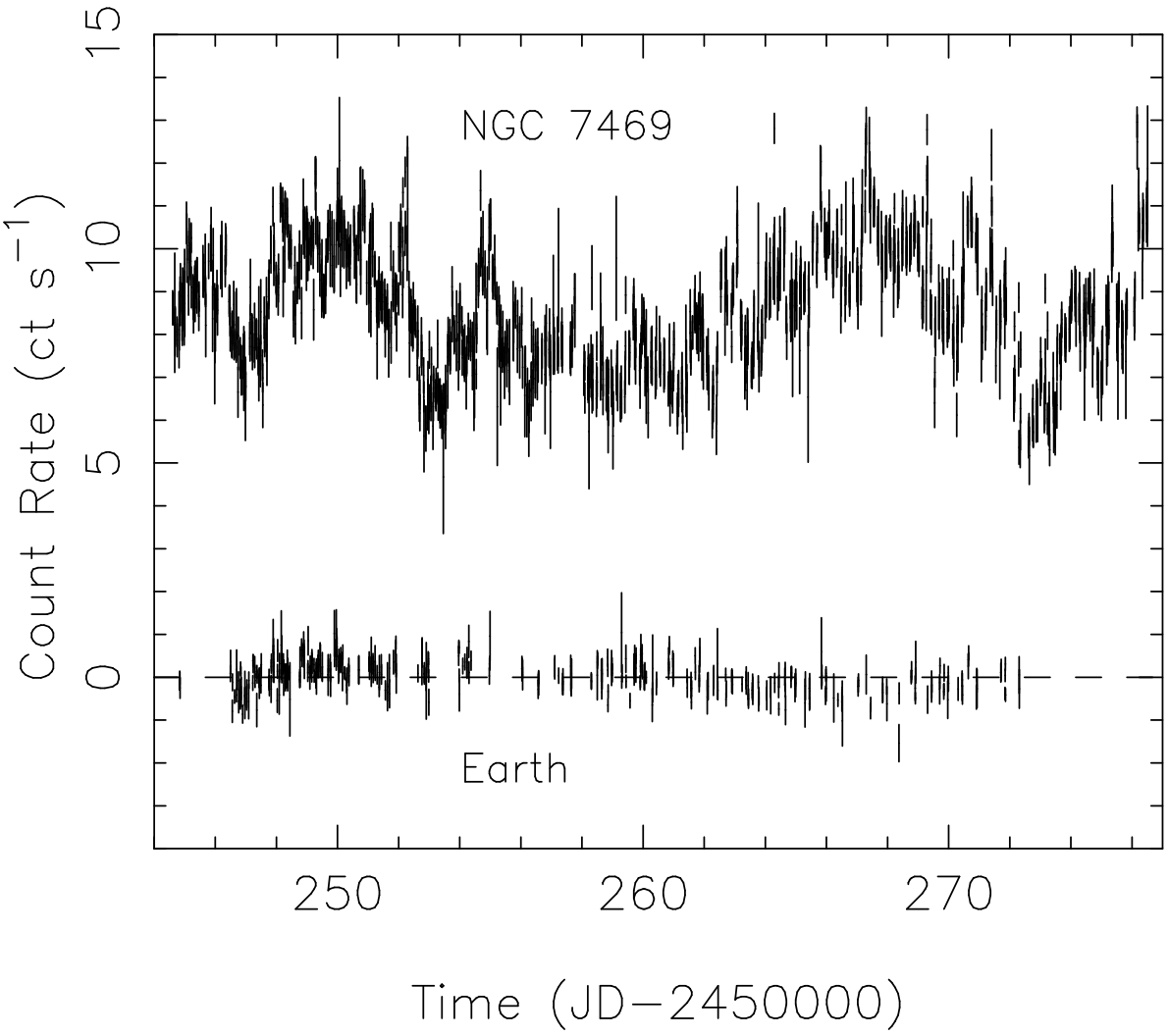

Fig. 1.— X-ray light curve (*RXTE*, 3 PCUs, 2-10 keV), after background subtraction, binned at 512s time resolution (upper points). The lower points show the background-subtracted light curve of the earth-occulted data. These data provide an estimate of the quality of the subtraction of the particle background for the *RXTE*/PCA. The dashed lines shows the zero count rate level, with which the earth-occulted data should be consistent after background subtraction. Those data show only small-amplitude variations (on relatively long time scales) which show clearly that the variations in the light curve on NGC 7469 are real, and not an artifact of poor background subtraction.

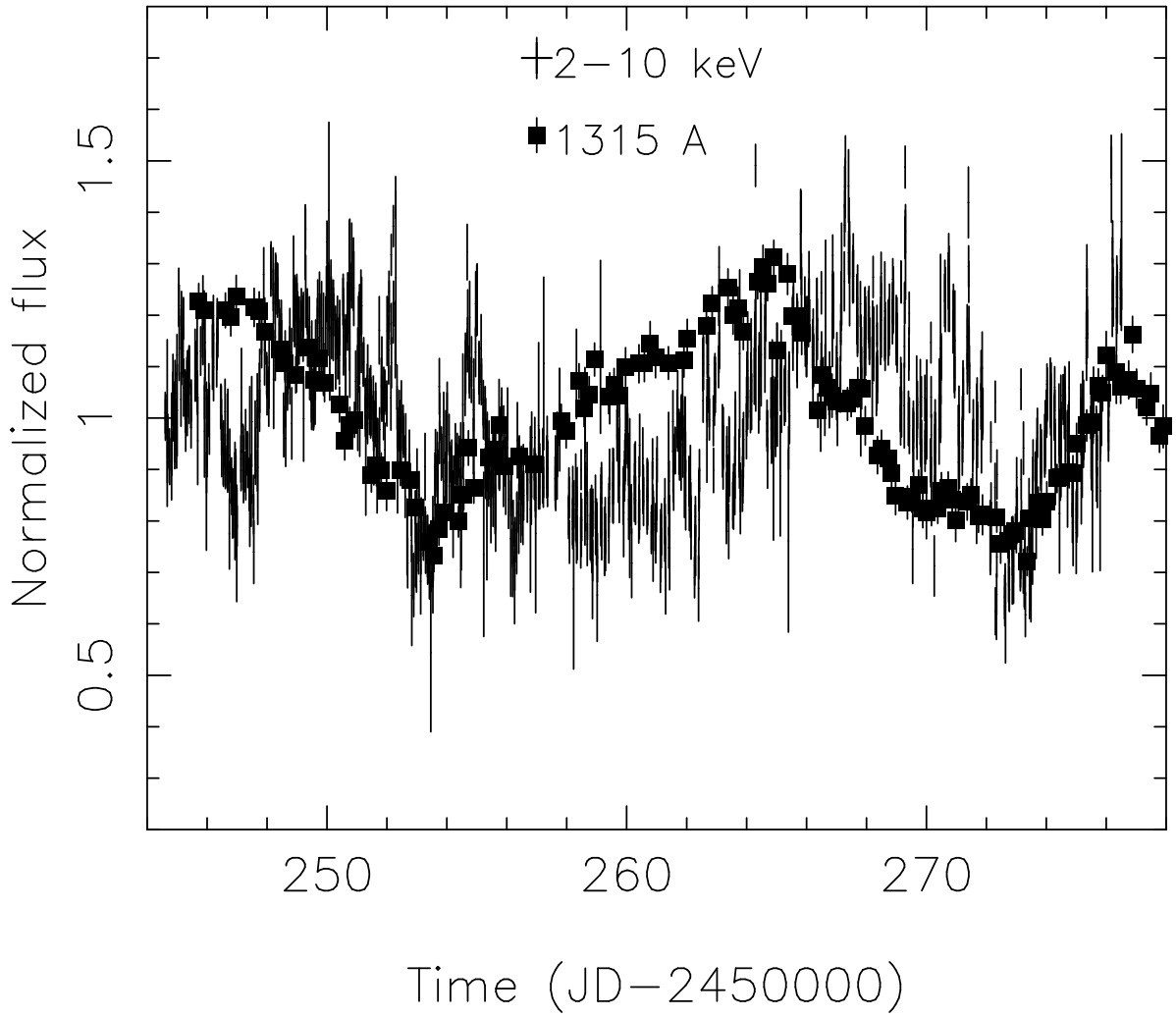

Fig. 2.— X-ray light curve (*RXTE* PCA, 2-10 keV) binned at 512s time resolution (crosses) together with the *IUE* 1315Å light curve in the UV (squares; W97). Both light curves have been normalized to their mean value and are plotted on the same time axis. We note the remarkable similarity in the amplitudes of variability on long time scales, but clear evidence for more rapid X-ray variations which are not observed in the UV. The light curves are not well correlated at zero lag, but the two prominent troughs appear to line up rather well in the time domain. In contrast, the apparent peaks in the UV light curve appear to precede the X-ray peaks.

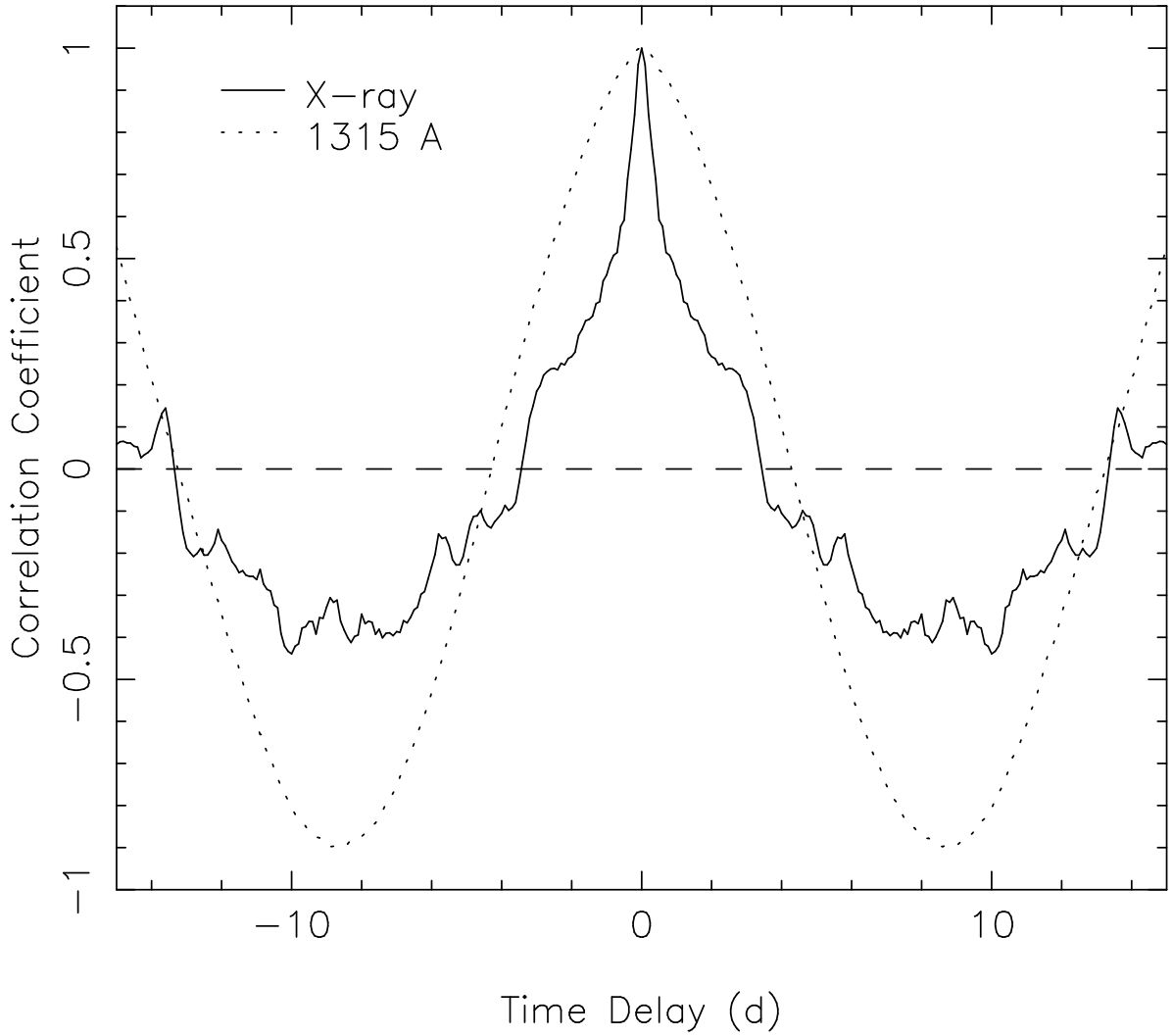

Fig. 3.— Auto-correlation functions of the X-ray (solid line) and UV 1315Å (dotted line) light curves. The X-ray ACF is much narrower (FWHM= 1.7 d) than that in the UV (FWHM = 5.3 d), illustrating the rapid variability which is not observed in the UV.

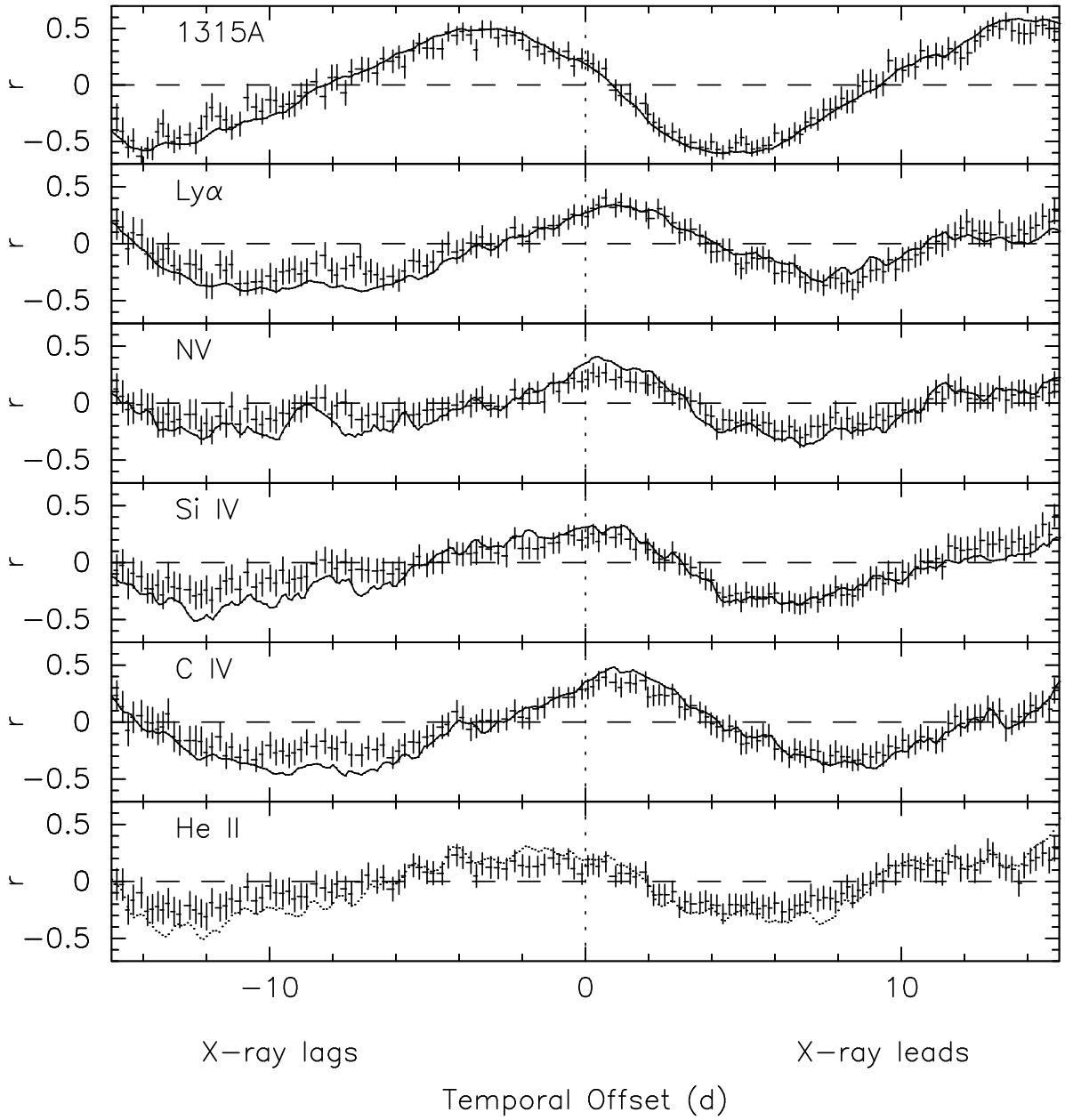

Fig. 4.— Cross-correlation functions for the X-ray light curve versus various UV light curves. In all cases the crosses represent the ZDCF (Alexander 1997) and the solid lines the ICCF (White & Peterson 1994). The top panel shows the correlation of the 2-10 keV X-rays with the continuum at 1315Å. The zero-lag correlation is rather weak, but a peak at a lag of ~ -4d and a trough at ~ 4d both have apparently high statistical significances. The UV emission lines (bottom five panels) are moderately well-correlated with the X-ray continuum. Indeed Lyα, Nv and Civ all correlate better with the X-ray continuum than the 1315Å continuum at zero lag. However, if a lag is allowed, the UV continuum is more strongly correlated.

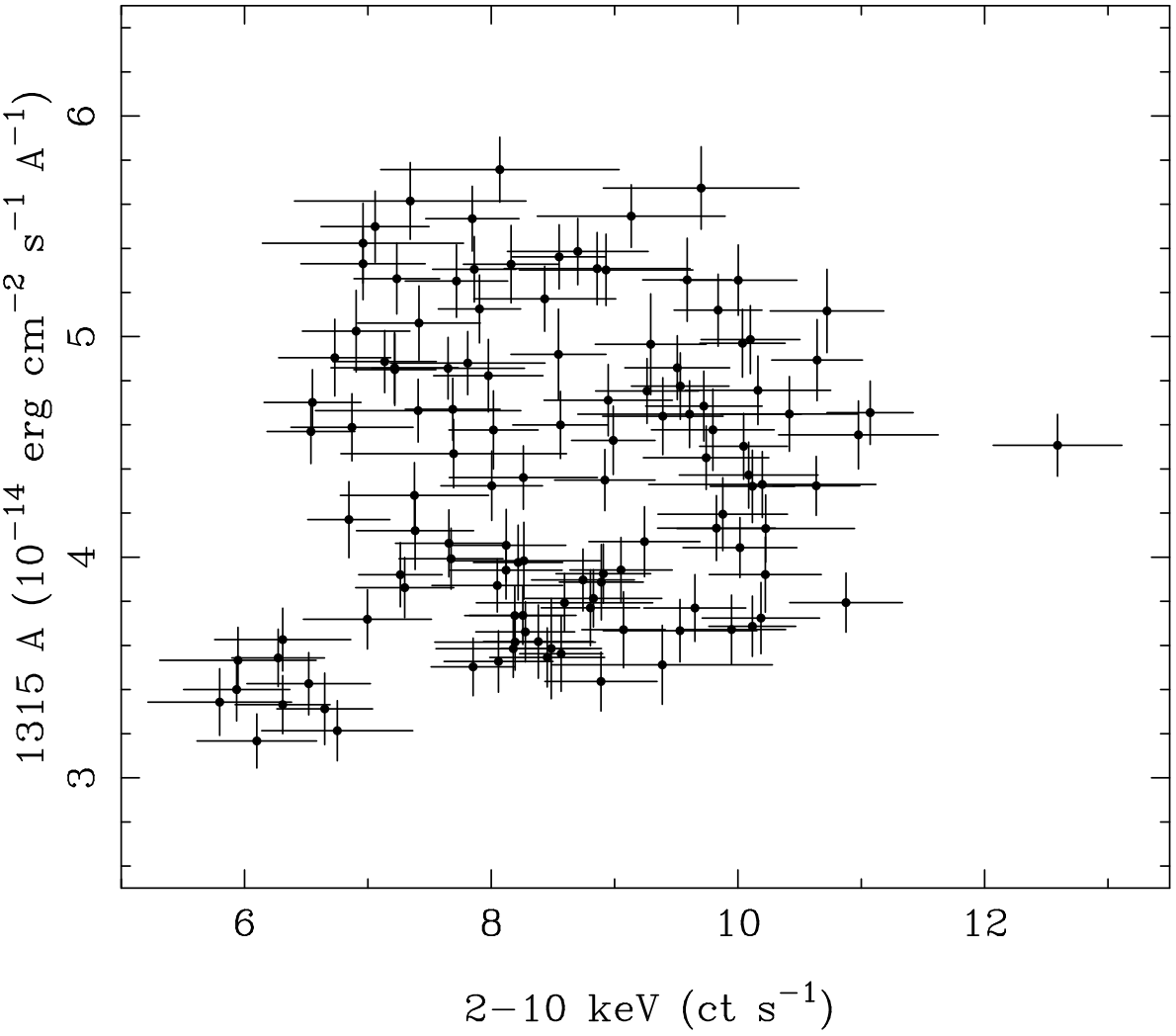

Fig. 5.— Estimated correlation of the X-ray count rate and UV flux. Pseudo-simultaneous X-ray data were estimated by interpolating the X-ray light curve to the times when the UV points were obtained. The correlation coefficient at zero lag, estimated from the ZDCF (Fig. 4) is found to be $r_0 = 0.19$, which is significant at 96 per cent confidence. The ICCF suggests a correlation coefficient of $r_0 = 0.16$, which is not significant. The correlation coefficient of the points shown is $r_0 = 0.15$ for 123 points, again not significant.

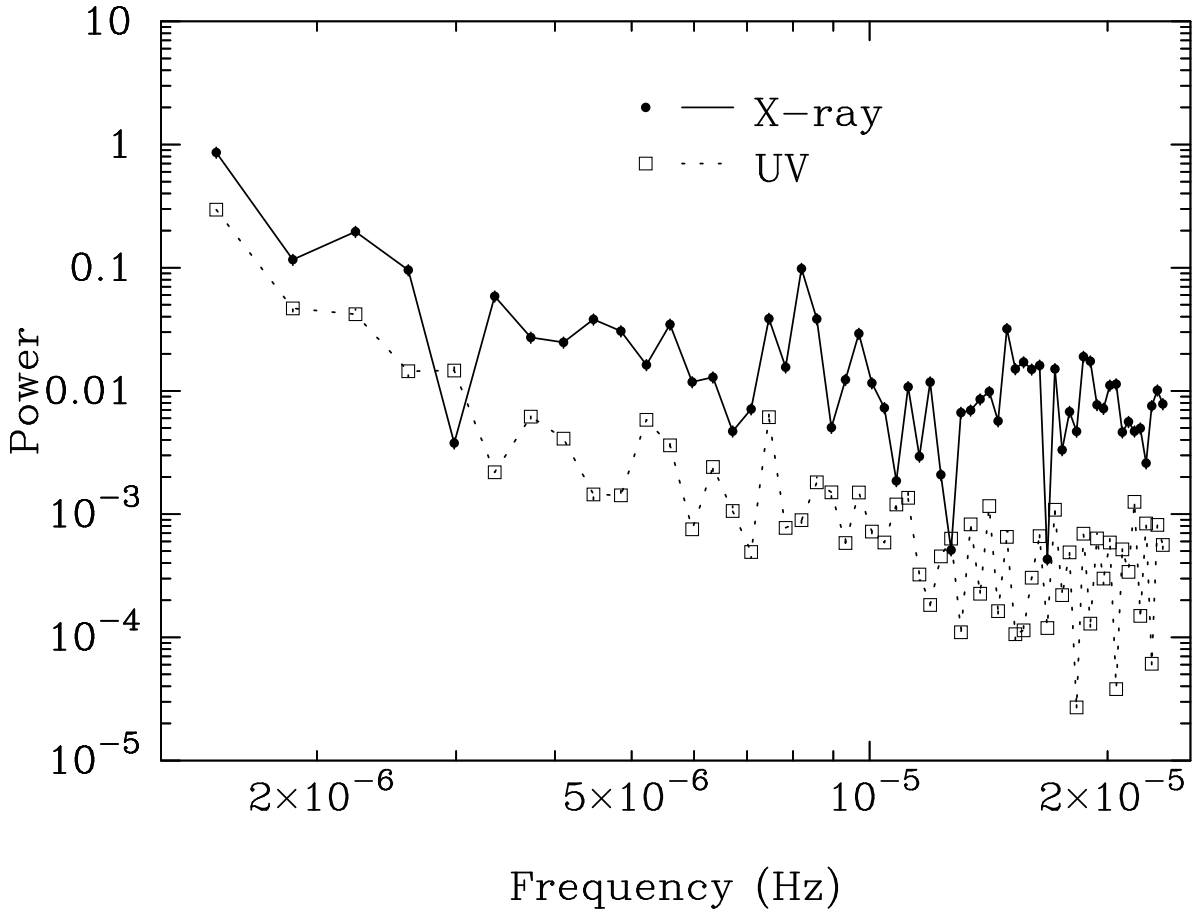

Fig. 6.— Periodograms for the X-ray (solid circles, solid line) and UV (open squares, dotted line) light curves. Both show a "red-noise" PDS without any obvious characteristic variability time scale. At face, value the power spectral slopes appear to be similar, although the X-rays show larger amplitude variations. However, significant statistical noise in the UV may make that PDS look artificially flat.

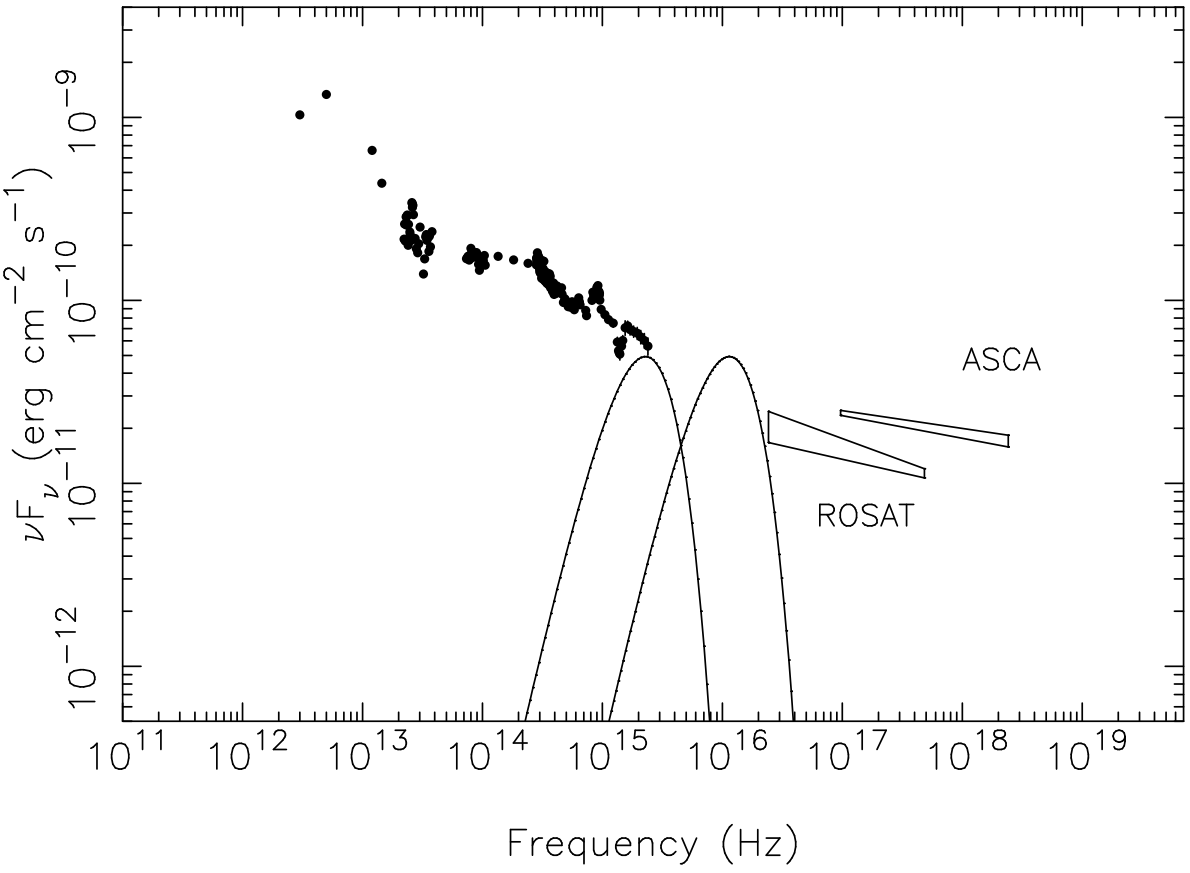

Fig. 7.— Spectral Energy Distribution for NGC 7469 from far-infrared to X-ray frequencies. The data are not simultaneous. The UV-to-far IR data were assembled from several instruments by Edelson & Malkan (1986) and references therein. The X-ray flux level observed here with *RXTE* was very similar to that seen by *ASCA*(Nandra et al. 1997; George et al. 1998). ROSAT data are from Brandt et al. (1993). The UV emission is similar to the mean observed here. The two solid lines shown are black body spectra with temperatures of 2 eV and 12 eV, and luminosity of 8×10^{43} erg s^{-1}. This represents our best estimate of the likely level of reprocessed X-ray flux in NGC 7469. The cooler blackbody is optimized to peak at 1315Å, and shows that reprocessed X-rays are just sufficient to account for the observed 1315Å flux. The 12 eV black body contributes only 5% of the flux at 1315Å and demonstrates that any X-rays reprocessed in NGC 7469 could plausibly be hidden in the EUV and soft X-ray bands, even if it is strongly peaked.

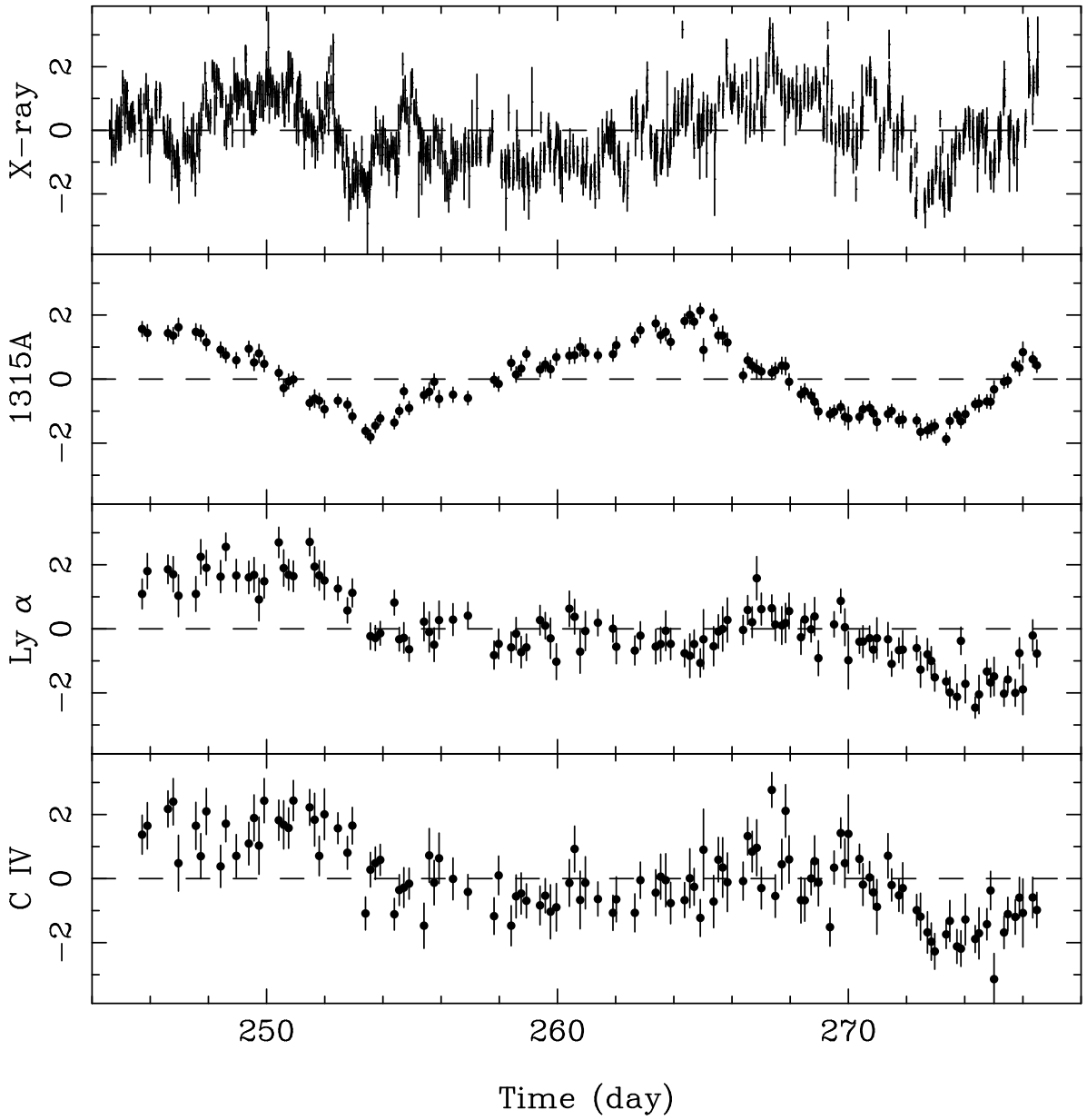

Fig. 8.— Light curves, renormalized to the rms variability parameter ($F_{\rm var}$) for (from top to bottom) the 2-10 keV X-rays, the 1315Å continuum, Lyα and CIV emission lines. The emission lines show a clear long-term fading which is not present in either continuum band.